

Orbits of Six Triple Systems

ANDREI TOKOVININ¹

¹*Cerro Tololo Inter-American Observatory — NSF's NOIRLab Casilla 603, La Serena, Chile*

ABSTRACT

Joint analysis of position measurements and radial velocities of six triple stellar systems is conducted to determine their inner and/or outer orbits. Accumulation of such data is needed to study the architecture of stellar hierarchies and its relation to the formation mechanisms. The inner periods in the six systems (HIP 11783, 64836, 72423, 84720, 89234, and 105404) range from 0.5 days to 44 yr. The shortest outer period of 3.34 yr is found in the compact triple HIP 105404 (BS Ind). The resolved triple system HIP 64836 has comparable inner and outer periods (5 and 30 yr), placing it near the limit of dynamical stability, while its quasi-circular and coplanar orbits suggest a 1:6 mean motion resonance. The periods in HIP 89234 (44 and \sim 450 yr) are also comparable, but the mutual orbit inclination is large, 54° . Masses of the components are estimated and each system is discussed individually.

1. INTRODUCTION

Many stars in the solar neighborhood, including the nearest one, α Cen, are arranged in hierarchical systems, believed to be a natural outcome of the star formation process. Almost every star could belong to a stellar system in its youth, at least for a while (Lee et al. 2019; Offner et al. 2023). Young dynamically unstable systems decay rapidly, but stable hierarchies survive for a long time, bearing an imprint of the formation history in their orbital architectures.

Separations in stellar systems span a huge range, from contact pairs to $\sim 10^4$ au and more. Their discovery and study is possible through combination of diverse and complementary methods, as no single technique can cover the full range. Space missions like TESS (Ricker et al. 2014) and Gaia (Gaia Collaboration et al. 2016, 2021) help us in finding new hierarchies, but suffer from various shortfalls when it comes to their detailed study. The major hurdle is to reach adequate time coverage and sampling. Dedicated ground-based programs address this need. In this paper, I use the results of high-resolution imaging and radial velocity (RV) monitoring to determine orbital parameters in six nearby triple systems; it continues our previous effort (Tokovinin & Latham 2017, 2020; Tokovinin 2021a, 2023a).

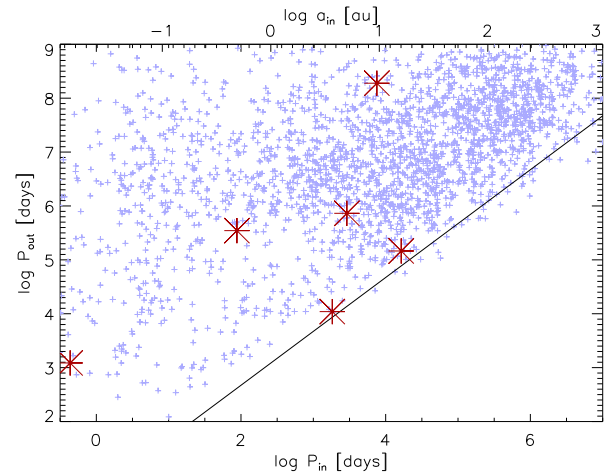


Figure 1. Inner and outer periods of known hierarchical systems within 100 pc (small crosses) and the six triple systems studied here (large asterisks). The line indicates the dynamical stability limit $P_{\text{out}}/P_{\text{in}} > 4.7$ (Mardling & Aarseth 2001). Some systems with crudely estimated periods are located below this line.

Basic parameters of the triple systems studied here are listed in Table 1. These stars are relatively bright and nearby, within 100 pc. To put this study into context, Figure 1 shows inner and outer periods of known hierarchies within 100 pc listed in the Multiple Star Catalog (MSC, Tokovinin 2018a). Only a minor fraction of these systems have known orbits (unknown periods are estimated roughly from projected separations). This study

Table 1. List of Multiple Systems

WDS	Name	HIP	HD	V	ϖ^a	μ_α^*	μ_δ	Masses
(J2000)				(mag)	(mas)	(mas yr ⁻¹)	(mas yr ⁻¹)	(M_\odot)
02321–1515	TOK 382	11783	15798	4.75	37.46 H	–72	–125	1.45+0.69
	BD–15 447	11759	15767	8.74	37.19 G	–73	–117	0.77
13175+2024	YSC 149	64836	...	11.06	17.45 G	–48	6	(0.65+0.63)+0.59
14485–1720	BU 346A	72423	130412	7.37	...	43	–54	1.21+0.48
	BU 346B	7.90	20.05 G	36	–46	1.10
17191–4638	41 Ara	84720	156274	5.48	113.75 G	1029	106	0.87
	LHS 445	8.69	113.87 G	953	140	0.60+0.42
18126–7340	HR 6751	89234	165259	5.85	23.68 G	–91	–254	1.47+0.73
	HDO 284B	9.28	23.71 G	–62	–241	0.82
21210–5229	BS Ind	105404	202947	8.91	19.00 D	40	–94	0.85+(0.77+0.55)

^a Parallax codes: G — Gaia DR3 (Gaia Collaboration et al. 2021), H — Hipparcos (van Leeuwen 2007), D — dynamical.

NOTE—Explanation of columns: (1) WDS code (Mason et al. 2001); (2) WDS or other name (3) Hipparcos number; (4) HD number; (5) visual magnitude; (6) parallax; (7) PM in R.A.; (8) PM in decl.; (9) masses.

contributes ten inner and/or outer orbits in six systems spanning a wide range of periods (large asterisks).

The input data and methods are briefly introduced in section 2. Sections 3–8 are devoted to individual systems, section 9 contains the summary.

2. DATA AND METHODS

2.1. Speckle Interferometry

In the hierarchies studied here, subsystems have been discovered or resolved by speckle interferometry with the high-resolution camera (HRCam) working on the 4.1 m SOAR (Southern Astrophysical Research Telescope) located in Chile. The instrument, data processing, and performance are covered in Tokovinin et al. (2010); Tokovinin (2018b). The latest series of measurements and references to prior observations can be found in Tokovinin et al. (2024). Image cubes of 200×200 pixels and 400 frames are recorded mostly in the y (543/22 nm) and I (824/170 nm) filters with an exposure time of 25 ms and a pixel scale of 15 mas. In the y filter, the diffraction-limited resolution of 30 mas can be attained, and even closer separations can be measured via careful data modeling. On the other hand, the I filter offers a deeper magnitude limit and a better sensitivity to faint, red companions.

Image cubes are processed by the standard speckle method based on calculation of the spatial power spectrum and image auto-correlation function (ACF) derived from the latter. The 180° ambiguity of position angles inherent to this method is resolved by examination of the shift-and-add (“lucky”) images and by comparison with prior data. In a triple star, the angles of subsystems are related, so the better-defined orientation

of the outer pair constrains the orientation of the inner subsystem.

For the outer pairs discovered visually, position measurements at SOAR are complemented by the historic micrometer and speckle data retrieved from the Washington Double Star (WDS) database (Mason et al. 2001) on my request.

2.2. Radial Velocities

Radial velocities of multiple systems come from various sources. Some stars were targeted by the CHIRON high-resolution optical echelle spectrometer at the 1.5 m telescope located at Cerro Tololo (Tokovinin et al. 2013). The spectra with a resolving power of 80,000 were processed by the instrument pipeline and cross-correlated with a binary mask based on the solar spectrum, as described in Tokovinin (2016). The resulting cross-correlation function (CCF) is approximated by one or two Gaussians to derive the RVs and other parameters, namely the amplitude and width of the CCF dips.

Reduced spectra of two targets obtained with the FEROS fiber echelle spectrograph (Kaufer & Pasquini 1998) at the 2.2 m telescope were downloaded from the ESO science archive. The spectral resolution is 48,000. These spectra were cross-correlated with the same solar-type mask to determine the RVs.

The RVs of HIP 72423 (HD 130412) have been monitored as part of the survey of nearby solar-type stars conducted at the Harvard-Smithsonian Center for Astrophysics (CfA) using several instruments on different telescopes. The instruments and data reduction methods are described in our previous papers (Tokovinin & Latham 2017, 2020).

2.3. Distances and Masses

The Gaia data release 3 (DR3, Gaia Collaboration et al. 2021) gives accurate astrometry based on 3 years of data. For close binary stars, the astrometry in DR3 is either missing or biased by the unmodeled orbital motions. Questionable astrometry is evidenced by large parallax errors and large values of the Reduced Unit Weight Error (RUWE) parameter. The bias is reduced for the orbital or acceleration solutions in the Gaia non-single star catalog (Gaia Collaboration et al. 2022). Otherwise, accurate parallaxes of distant non-binary components of triple systems should be used. In some cases, the shorter time base of Gaia DR2 gives less biased parallaxes because the orbital motion was closer to linear.

The masses of the components are estimated from their absolute magnitudes M_V using standard relations for main sequence dwarfs (Pecaut & Mamajek 2013). The combined flux is distributed between the unresolved components in suitable proportion, guided by the magnitude differences measured by speckle interferometry or by other arguments. This relative photometry is not very accurate (typical scatter of 0.1 mag or more in the I band). Lacking accurate differential photometry in several bands, the adopted flux ratios in V are only approximate; however, considering the strong dependence of M_V on mass, the “photometric” masses are determined reasonably well. They are checked against the mass sum derived from well-determined orbits and parallaxes.

2.4. Orbit Calculation

As in the previous papers, an IDL code `orbit3` that fits simultaneously inner and outer orbits in a triple system to available position measurements and RVs has been used (Tokovinin 2017).¹ The method is presented in Tokovinin & Latham (2017). The weights are inversely proportional to the squares of adopted measurement errors which range from 2 mas to 0.05 and more (see Tokovinin 2021a, for further discussion of weighting).

Motion in a triple system can be described by two Keplerian orbits only approximately, but the effects of mutual dynamics are too small to be detectable with the current data. The code fits 14 elements of both orbits and the additional parameter f – the wobble factor, ratio of the astrometric wobble axis to the full axis of the inner orbit. For resolved triples, $f = q/(1+q)$, where q is the inner mass ratio. When the inner subsystem is

not resolved, measurements of the outer pair refer to the photocenter of the inner pair, and the wobble amplitude corresponds to a smaller factor $f^* = q/(1+q) - r/(1+r)$, where r is the flux ratio. The code `orbit4` can accept a mixture of resolved and unresolved outer positions; it adopts a fixed ratio f^*/f , specified for each system as an input parameter.

To avoid the degeneracy of outer orbits resulting from insufficient time coverage, some elements are fixed to reasonable values that agree with the estimated masses. The resulting outer orbits are only representative; however, they are useful for the assessment of mutual dynamics.

The elements of inner and outer orbits in the selected triple systems are given in Table 2 in standard notation. Considering the uncertain nature of some outer orbits, the formal errors of their elements are only lower limits. When both positions and RVs are available, the argument of periastron ω_A is chosen to represent the RVs of the primary component, and the node Ω_A gives correct positions of the secondary; adding 180° to both elements does not affect the positions.

Individual positions, their adopted errors, and residuals to the orbits are listed in Table 3, available in full electronically. The systems are identified by their WDS codes (their HD and HIP numbers are given in Table 1) and components. Compared to the published HRCam data, the positions are corrected for the small systematics determined in Tokovinin et al. (2022) and, in a few cases, re-processed. The second column indicates the subsystem; for example, A,BC refers to the angle and separation between A and unresolved pair BC, while A,B refers to the position of the resolved component B relative to A. The RVs and their residuals to orbits are listed in the electronic Table 4. Larger errors are assigned to some RVs to down-weight their impact on the orbit, as commented in the following sections.

3. HIP 11783 (σ CET)

This triple system is located at 27 pc distance. The bright primary component A (σ Cet, HR 740, HIP 11783, $V = 4.75$ mag, F5V) and star B (HIP 11759, HD 15767, $V = 8.74$ mag, K2.5V) at $345''$ form a wide common proper motion (CPM) pair designated as GWP 335AB in the WDS with an estimated period of ~ 500 kyr. The most accurate distance to the system re-

¹ Codebase: <http://dx.doi.org/10.5281/zenodo.321854>

Table 2. Orbital Elements

WDS	System	P	T	e	a	Ω_A	ω_A	i	K_1	K_2	V_0
HIP		(yr)	(yr)		($''$)	(degr)	(degr)	(degr)	(km s^{-1})	(km s^{-1})	(km s^{-1})
02321–1515	Aa,Ab	20.68	2015.621	0.854	0.3616	23.1	23.4	120.3	7.56	...	–28.85
11783		± 0.670	± 0.055	± 0.009	± 0.0049	± 1.3	± 2.6	± 1.3	± 0.25	...	± 0.10
13175+2024	Aa,Ab	5.000	2022.84	0.285	0.050	292.6	6.6	134.0	6.99	7.33	...
64836		± 0.052	± 0.08	± 0.020	± 0.002	± 4.1	± 9.1	fixed	± 0.34	± 0.35	...
13175+2024	A,B	30.00	2005.16	0	0.207	295.2	0	143.2	2.3	...	–7.0
64836		± 0.28	± 1.08	fixed	± 0.017	± 2.6	fixed	± 1.6	fixed	...	fixed
14485–1720	Aa,Ab	7.948	2023.804	0.642	0.0270	262.4	164.6	40.0	4.17
72423		± 0.017	± 0.034	± 0.036	± 0.0013	± 3.5	± 4.6	fixed	± 0.40
14485–1720	A,B	2000	1368	0.262	4.60	125.0	337.1	75.1	1.40	2.15	1.55
72423		fixed	± 40	± 0.026	fixed	± 1.1	± 4.5	± 0.6	fixed	fixed	± 0.06
17191–4638	Ba,Bb	0.24069	2015.903	0.773	0.0410	242.2	170.6	57.9
...		fixed	± 0.012	fixed	± 0.0024	± 14.8	± 31.1	± 4.9
17191–4638	A,B	954.2	1908.2	0.816	12.752	320.2	150.3	35.2	1.956
84720		± 68.7	± 0.28	± 0.007	± 0.548	± 2.5	± 1.3	± 0.8	± 0.068
18126–7340	Aa,Ab	44.2	2027.22	0	0.373	105.2	0	83.5
89234		± 1.3	± 0.32	fixed	± 0.008	± 0.3	fixed	± 0.4
18126–7340	A,B	450	2147.2	0.300	2.014	65.3	348.8	46.7
89234		fixed	± 21.8	fixed	± 0.051	± 9.1	± 23.0	± 1.6
21210–5229	A,B	3.3473	2020.583	0.627	0.0552	248.72	357.12	42.35	13.76	...	10.62
105404		± 0.0015	± 0.007	± 0.006	± 0.0005	± 0.69	± 0.90	± 2.13	± 0.36	...	± 0.06

Table 3. Position Measurements and Residuals (Fragment)

WDS	Syst.	Date	θ	ρ	σ_ρ	$(O-C)_\theta$	$(O-C)_\rho$	Method ^a
		(JY)	($^\circ$)	($''$)	($''$)	($^\circ$)	($''$)	
02321–1515	Aa,Ab	2013.7461	162.0	0.2090	0.005	–0.2	0.000	S
02321–1515	Aa,Ab	2014.0410	157.4	0.1774	0.005	–0.1	0.000	S
02321–1515	Aa,Ab	2014.0410	158.2	0.1768	0.005	0.7	–0.001	S
02321–1515	Aa,Ab	2016.9572	214.9	0.2389	0.005	0.8	0.001	S

^a Methods: G: Gaia; H: Hipparcos; M: visual micrometer measurement; P: photographic measurement; S: speckle interferometry at SOAR; s: speckle interferometry at other telescopes.

Table 4. Radial Velocities and Residuals (Fragment)

WDS	Comp.	JD	RV	σ	$(O-C)$	Instr. ^a
		(JD – 24,000,000)	(km s^{-1})	(km s^{-1})	(km s^{-1})	
02321–1515	Aa	52594.500	–29.50	2.00	0.64	T2005
02321–1515	Aa	52597.500	–29.00	2.00	1.14	T2005
02321–1515	Aa	52600.500	–29.80	2.00	0.34	T2005
02321–1515	Aa	54706.6040	–29.45	0.50	–0.17	RAVE
02321–1515	Aa	56908.8810	–24.58	0.10	0.00	CHI
02321–1515	Aa	57389.0000	–26.82	3.89	–0.33	DR2

^a Instruments: CHI: CHIRON; CfA: CfA digital speedometers; COR: CORAVEL; DR2: Gaia DR2; G2005: Guenther et al. (2005); FEROS: FEROS; RAVE: Steinmetz et al. (2020); TRES: TRES; T2005: Takeda et al. (2005).

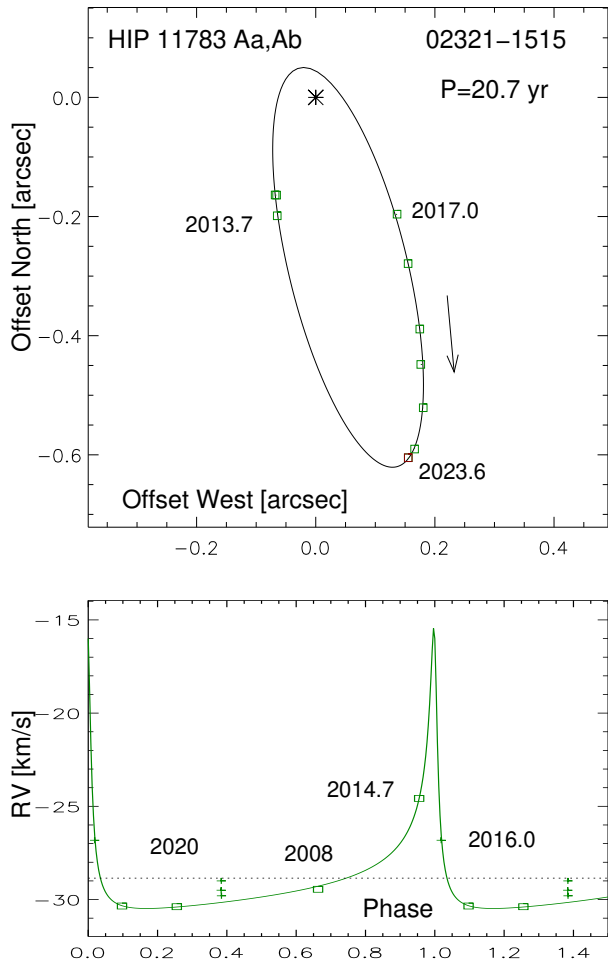


Figure 2. Orbit of HIP 11783 Aa,Ab in the plane of the sky (top) and its RV curve (bottom). Squares plot the measurements, the curves depict the orbits. Crosses in the RV curve mark the less accurate RVs.

sults from the Gaia DR3 parallax of star B, 37.19 ± 0.02 mas. It matches the HIP2 (van Leeuwen 2007) parallax of star A, 37.46 ± 0.25 mas, while the Gaia astrometry of A is strongly biased by its orbital motion near the periastron (e.g. a parallax of 43.38 ± 0.56 mas in DR3). The PM of A listed in Table 1 is estimated by Brandt (2018) from positions in Hipparcos and Gaia DR2; it is slightly biased, but closer to reality than the Gaia PM.

The bright star A has an extensive literature. The spectroscopy, summarized in Soubiran et al. (2010), indicates an effective temperature of 6300 K, a surface gravity $\log g$ from 3.7 to 4.0 (slightly evolved), and a metallicity of -0.30 to -0.25 dex. Star A is known to have a variable RV (Nordström et al. 2004) and astrometric acceleration (Makarov & Kaplan 2005). Its faint companion Ab was resolved for the first time at SOAR in 2013.7 at $0''.2$ separation with a large contrast (aver-

age $\Delta I = 3.89$ mag with an rms scatter of 0.17 mag); it is designated as TOK 382Aa,Ab in the WDS.

The RVs of A and B were measured in 2014.7 using CHIRON and found to be substantially different. At that time, the pair Aa,Ab was approaching periastron of its eccentric orbit and it became unresolved at SOAR after 2014. The RVs and positions measured after the periastron allowed calculation of an orbit with a period of 21 yr (Tokovinin 2021b). The orbital elements are updated here using recent speckle measurements and RVs (Figure 2). Despite the large contrast, the rms residuals to the orbit are less than 2 mas. Crosses on the RV curve denote RVs used with a low weight, namely three points from Takeda et al. (2005) and the mean RV in Gaia DR3. The latter has a large error of 3.89 km s^{-1} owing to the rapid RV variation near periastron. One RV from RAVE DR6 (Steinmetz et al. 2020) measured in 2008 is also used. When the RV series from Gaia become publicly available in DR4, they can be used to improve the orbit; the next periastron in 2036 will present another chance to cover it spectroscopically.

The Gaia DR3 parallax of B and the orbit of Aa,Ab correspond to the mass sum of $2.15 M_{\odot}$. Adopting the mass of $1.45 M_{\odot}$ for Aa, the RV amplitude and inclination lead to a mass of $0.70 M_{\odot}$ for Ab, matching the mass sum. The mass of the CPM companion B estimated from its absolute magnitude is $0.77 M_{\odot}$. Its mean RV of -28.23 km s^{-1} is very close to the center-of-mass velocity of A, -28.85 km s^{-1} . The CHIRON spectrum of B shows no lithium 6707 \AA line, while in the spectrum of A it is prominent (equivalent width 78 m\AA). The axial rotation of A estimated from the CCF width is moderate, $V \sin i = 7 \text{ km s}^{-1}$.

4. HIP 64836 (YSC 149)

The K5V dwarf HIP 64836 (WDS J13175+2024, $V = 11.06$ mag) is located in the solar vicinity (GJ 9436, MCC 687). The Gaia DR3 parallax is 17.45 ± 0.45 mas, with a RUWE of 30. The Hipparcos (van Leeuwen 2007) gives a stochastic solution with a parallax of 16.69 ± 2.57 mas. Horch et al. (2012) resolved this star in 2008.47 into a $0''.2$ pair YSC 149. Their subsequent observations in 2012.09 and 2014.46 revealed this as a triple system where the secondary component is a close pair Ba,Bb with a separation of 50 mas (Horch et al. 2015, 2017).

Observations of this system at SOAR in 2016, 2018, and 2019 produced measurements of the A,B pair without resolving the subsystem. The latter was clearly resolved in 2021.16 and marginally resolved in 2022–2024. The SOAR data indicate that the subsystem belongs to the primary: it is Aa,Ab rather than Ba,Bb. This con-

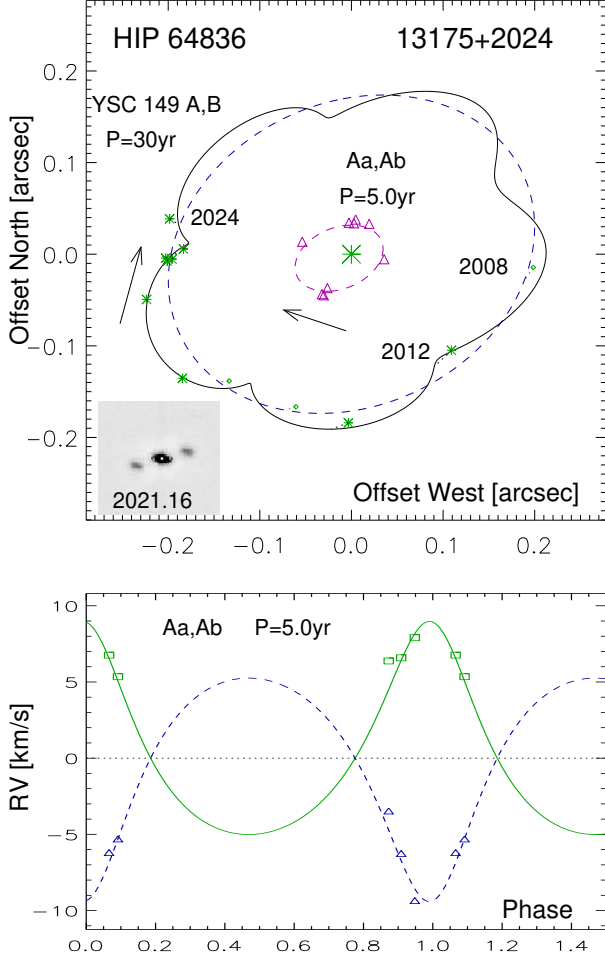


Figure 3. Orbits of HIP 64836 (YSC 149) in the plane of the sky (top) and the RV curve of the inner pair (bottom, the outer orbit is subtracted). In the orbit plot, asterisks, crosses, and triangles show the resolved outer, unresolved outer, and inner positions, respectively. The inner orbit is plotted by the small dashed ellipse. The outer orbit is plotted by the solid line (with wobble) and by the dashed line (with wobble removed). The insert shows the speckle ACF recorded in 2021.

clusion is supported by the relative photometry. Star B is fainter than A by 1.43 mag in the V band (Horch et al. 2012) and by 1.1 mag in I (SOAR). Yet, in 2012 Horch et al. measured magnitude differences of Ba and Bb relative to A of 0.62 and 0.67 mag (at 692 nm), implying that the combined light of Ba and Bb exceeds the light of A. Their photometry in 2014 again suggests that B is brighter than A. If B were a pair of similar stars, each of them should be ~ 1.8 mag fainter than A.

Attributing the subsystem to A leads to the V magnitudes of Aa, Ab, and B of 11.97, 12.18, 12.42 mag (assuming $\Delta V_{A,B} = 1.43$ mag and $\Delta V_{Aa,Ab} = 0.2$ mag). Given the DR3 parallax and the standard mass-luminosity relation (Pecaut & Mamajek 2013), these

magnitudes correspond to the masses of 0.65, 0.63, and $0.59 M_{\odot}$ (mass sum $1.85 M_{\odot}$). All three stars in this system are therefore late-K dwarfs.

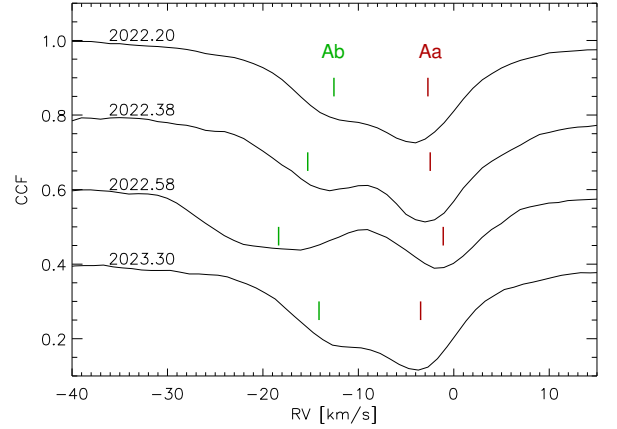


Figure 4. Four CCFs of HIP 64836 derived from the CHIRON spectra. The dates are indicated. The color ticks mark the measured heliocentric RVs of Aa (red, on the right) and Ab (green).

The separations imply the inner and outer periods of the order of 5 and 30 yr, respectively. About half of the outer orbit is covered. I averaged the positions of A,Ba and A,Bb reported by Horch et al. to get the “unresolved” positions of A,B and fitted a preliminary outer orbit. Independently, B. Mason computed a preliminary outer orbit of YSC 149 with a period of 32.96 yr (Tokovinin et al. 2024). Guessing the orbit of the inner subsystem Aa,Ab was less obvious because the period is short, the magnitude difference is small ($\Delta I_{Aa,Ab} = 0.15$ mag with rms scatter of 0.11 mag), and the separation of Aa,Ab is always near the diffraction limit. This allows swaps between Aa and Ab. The SOAR observations in 2016.13 and 2019.38 were reprocessed using the triple-star model. The data suggest retrograde motion of the inner pair with a period of ~ 5 yr.

The estimated RV amplitude in the inner pair is ~ 5 km s $^{-1}$, so triple lines could possibly be detected in high-resolution spectra. The resolution of three CORAVEL observations reported by Sperauskas et al. (2016) is not high enough to detect triple lines. Four spectra were taken with CHIRON. The CCFs look double-lined (Figure 4). The stronger dip on the right side (red tick marks) is identified here with Aa, and the left-side dip (green ticks) with Ab. Against expectation, the CCF is not triple-lined, possibly because the weakest star B is a fast rotator with shallow lines. I recovered from the ESO science archive one spectrum taken with FEROS in 2023 March (JD 2,460,007.7544, program led by E. Costa). Another FEROS spectrum

taken by E. Costa on my request in 2024 April (JD 2,460,420.651) shows only one blended CCF dip with an RV of -7.33 km s^{-1} which is not used in the orbit fit, but matches its prediction.

The inner and outer positions and RVs were fitted jointly using `orbit4`. Regarding the alternative outer positions measured by Horch et al. in 2012 and 2014, I selected those that match the joint orbits (Table 2). Figure 3 shows both orbits. The resolved outer positions Aa,B are plotted as asterisks, the unresolved A,B as small crosses, and the dashed line shows the outer orbit without wobble. The fitted wobble factor $f = 0.41 \pm 0.05$ corresponds to the inner mass ratio $q_{\text{in}} = 0.75 \pm 0.15$, the RV amplitudes indicated $q_{\text{in}} = 0.71$, contradicting the near-equality of stars Aa and Ab. A closer examination of the data shows that the individual RV amplitudes of Aa and Ab are constrained weaker than their sum, so both the spectroscopic mass ratio and the wobble amplitude are somewhat uncertain. In the final iteration, I fixed $f = 0.49$, the outer RV amplitude $K_3 = 2.3 \text{ km s}^{-1}$, and the center of mass velocity $V_0 = -7.0 \text{ km s}^{-1}$ to get nearly equal RV amplitudes in the inner orbit. The free fit yields the inner inclination of $i_{\text{in}} = 135^\circ.1 \pm 5^\circ.3$, so $i_{\text{in}} = 134^\circ$ was fixed to match the RV amplitudes with the expected inner mass sum of $1.28 M_\odot$. The outer eccentricity is not significantly different from zero, so $e_{A,B} = \omega_{A,B} = 0$ were also fixed.

Overall, these orbits give a good match to the available observations and to the properties of normal low-mass stars. The mutual inclination between the orbits is $\Phi = 10^\circ.0 \pm 1^\circ.7$; the period ratio is 6.0 ± 0.1 , hinting at a 6:1 mean motion resonance. This triple system resembles some other low-mass hierarchies with similar architecture (quasi-circular and coplanar orbits, comparable masses, small period ratio), such as the triple system 00247–2653 or LHS 1070 (Tokovinin 2018c), where the latest speckle data correspond to the inner and outer periods of 17.26 ± 0.02 and $83.0 \pm 1.8 \text{ yr}$, respectively, and their ratio is 4.8 ± 0.1 .

For a test, the outer orbit was fitted separately by using outer positions corrected for the inner subsystem, the mean RVs of Aa and Ab, and the less accurate blended RVs from Sperauskas et al. (2016) to extend the time coverage. This experiment confirmed the near-zero outer eccentricity and the adopted ascending node of the outer orbit.

The Gaia DR3 parallax of $17.45 \pm 0.51 \text{ mas}$ corresponds to the inner and outer mass sums of 0.95 and $1.85 M_\odot$, respectively. The Gaia astrometry is affected by the complex motion of the unresolved photocenter. Fitting Gaia transits by an acceleration or by a single Keplerian orbit will not be sufficient.

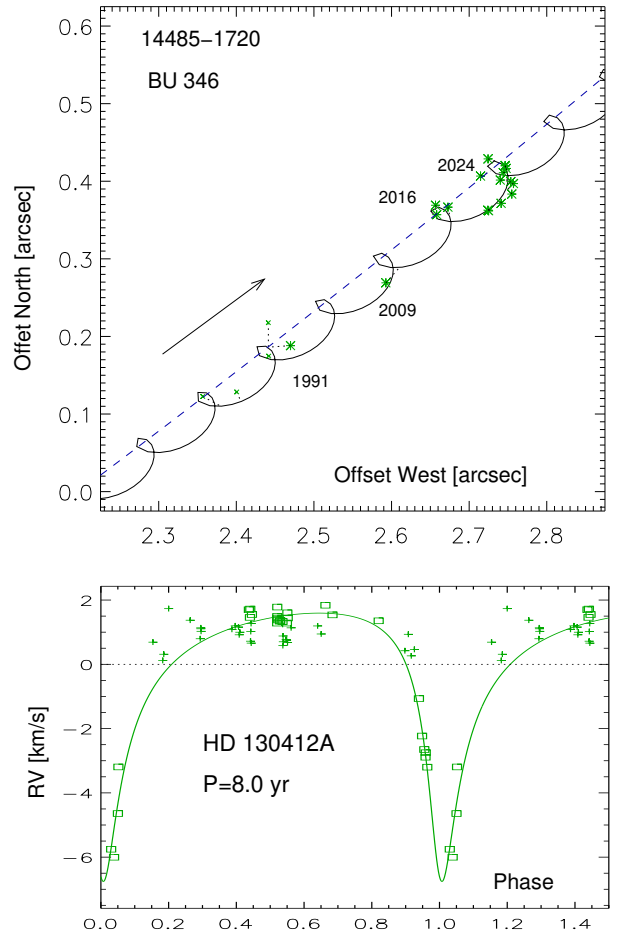


Figure 5. Top: fragment of the outer orbit with wobble. Accurate measurements (HIP, Gaia, SOAR) are plotted as asterisks, less accurate data by crosses. The dashed line depicts the center-of-mass trajectory. Bottom: the RV curve of star A. Plus signs denote RVs potentially biased by blending; the center-of-mass RV is subtracted.

5. HIP 72423 (HD 130412, BU 346)

The visual pair BU 346 (ADS 9387, WDS J14485–1720) has been resolved in 1875 at a separation of $1''$ (Burnham 1875). A slow and almost linear orbital motion was revealed during 1.5 centuries, and now the separation has increased to $2''.75$. Stars A and B have individual entries in the Gaia DR3 catalog, which gives no parallax for A and a parallax of $20.046 \pm 0.025 \text{ mas}$ for B. The DR2 catalog contains astrometry for both A and B, but the nonlinear motion of star A definitely disagrees with the Gaia default single-star model, explaining the absence of its parallax and proper motion (PM) in DR3. Gaia gives G magnitudes of 7.23 and 7.72 mag for A and B (or V of 7.37 and 7.86 mag). The masses of Aa and B are estimated as 1.2 and $1.1 M_\odot$ from their V -band absolute magnitudes using the DR3 parallax of B.

The RV of A has been monitored by the CfA team led by D. Latham since 1984 and found to be variable. According to the private notes, a tentative orbit with $P = 4.7$ yr has been determined but not published. After preliminary analysis of all available data in 2023 May, it became clear that the inner subsystem Aa,Ab was approaching periastron, and a fast RV variation was expected. In 2023 May–June, the system was observed twice with CHIRON and four times with the TRES spectrograph (Szentgyorgyi & Furész 2007). A negative RV trend was revealed, confirming the predicted periastron in 2023.7.

An orbit of A,B with $P = 1715.7$ yr and $a = 9''.407$ has been determined by Izmailov (2019) via formal least-squares fit to all measures collected in the WDS. With a parallax of 20.05 mas, it corresponds to the mass sum of $35 M_{\odot}$, hence it is unlikely to be correct. The outer orbit is poorly constrained by the short (42°) observed arc. The pair A,B was originally included in a set of calibrator binaries for SOAR speckle interferometry. For this reason, it was observed rather frequently. Accurate SOAR measurements show clearly a deviation from the linear motion (wobble). I assume that the wobble is produced by the subsystem in the component A, considering its variable RV.

The IDL code `orbit3` was used to simultaneously fit the positions of A,B and the RVs of A by two Keplerian orbits (Figure 5). The outer period and semimajor axis were fixed to values that give the estimated mass sum of $2.8 M_{\odot}$. The inner period was found to be about 8 yr. Inaccurate speckle measures by Horch on a 0.8 m telescope and the Washington speckle data from the 26 inch refractor are ignored, as well as many micrometer and photographic measures. The inner pair is never resolved, so the wobble factor is fixed to $f = 1$, and the resulting a_{in} is the astrometric axis.

D. Latham has communicated the RVs of A and B measured with CORAVEL, CfA digital spectrometers, and TRES, corrected to be on the same system (add $+0.14 \text{ km s}^{-1}$ to bring these RVs to the absolute system). In the final iteration of the orbits, these RVs were used. However, considering the small separation between A and B on the sky, their light can be frequently blended, biasing the RVs of A toward the RV of companion B (its mean RV is $+1.7 \text{ km s}^{-1}$). Attempting to resolve the visual pair, observers likely offset the object on the slit, also creating an RV bias. To avoid subjective selection, I assigned an increased error of 0.9 km s^{-1} to all CfA RVs between 0.6 and 2.6 km s^{-1} , assuming that they can be biased by blending; the remaining RVs were given the unmodified errors around 0.35 km s^{-1} . Some RVs of star B, apparently affected by

blending or misidentification with A, are also strongly down-weighted. The RVs measured with TRES and CHIRON are assigned errors of 0.2 km s^{-1} . The weighted residuals to the orbit are 0.35 km s^{-1} for Aa and 0.26 km s^{-1} for B. The weighted position residuals are 4 and 5 mas in X and Y and also match the assigned errors. The SOAR measurement errors are dominated by the calibration uncertainty. Figure. 1 in Tokovinin et al. (2022) suggests that the position errors of the calibrator binaries of similar separation are about 4 mas.

The free fit leads to a small inclination of the inner orbit, which would imply an unrealistically large mass of the companion Ab. So, the inner inclination was fixed at 40° , yielding a mass of $0.5 M_{\odot}$ for Ab. The joint fit of positions and RVs constrains the inner orbit much better than each of these data sets alone. The astrometric axis is 27.0 mas, while the full axis of the Aa,Ab orbit, computed from the mass sum and period, is 95.1 mas. Their ratio gives the wobble factor $f = 0.28$ and the mass ratio $q_{\text{Aa,Ab}} = 0.40$; if the mass of Aa is $1.21 M_{\odot}$, the mass of Ab is $0.48 M_{\odot}$.

Given that the data do not constrain well the outer orbit, a circular orbit with $P = 1900$ yr was fitted initially to the observed arc. However, it predicted a substantial (about 3 km s^{-1}) difference between the systemic RV of A and the RV of B, while they agree to within 1 km s^{-1} . The outer inclination is certainly large, while the estimated RV amplitudes in the outer orbit are 1 to 2 km s^{-1} . So, the small RV difference between A and B indicates that the outer pair is close to its node. The final solution with an outer eccentricity of 0.26 matches this additional constraint. The outer RV amplitudes were fixed to their values estimated from the adopted masses of A and B, 1.7 and $1.1 M_{\odot}$, and the joint fit was repeated several times. The results reported here refer to the final iteration. The outer orbit remains quite uncertain, but its elements describe well the observed motion.

Brandt (2018) detected a very large PM anomaly (PMA) of star A by comparing its Gaia DR2 astrometry with Hipparcos. However, considering that Gaia was affected by the inner orbit of star A, its comparison with the orbits can be only qualitative. If we take the accurate PM of star B measured in DR3, $(36.2, -47.0) \text{ mas yr}^{-1}$, and subtract the motion in the outer orbit, $(-9.9, +7.5) \text{ mas yr}^{-1}$, the resultant PM of star A, $(46.1, -54.5) \text{ mas yr}^{-1}$, is in reasonable agreement with the average DR2–HIP PM of $(43.2, -54.2) \text{ mas yr}^{-1}$ determined by Brandt. Deviations of the PM of A from its average PM in 1991.25 and 2015.5 predicted by the inner orbit approximately match the measured PMs.

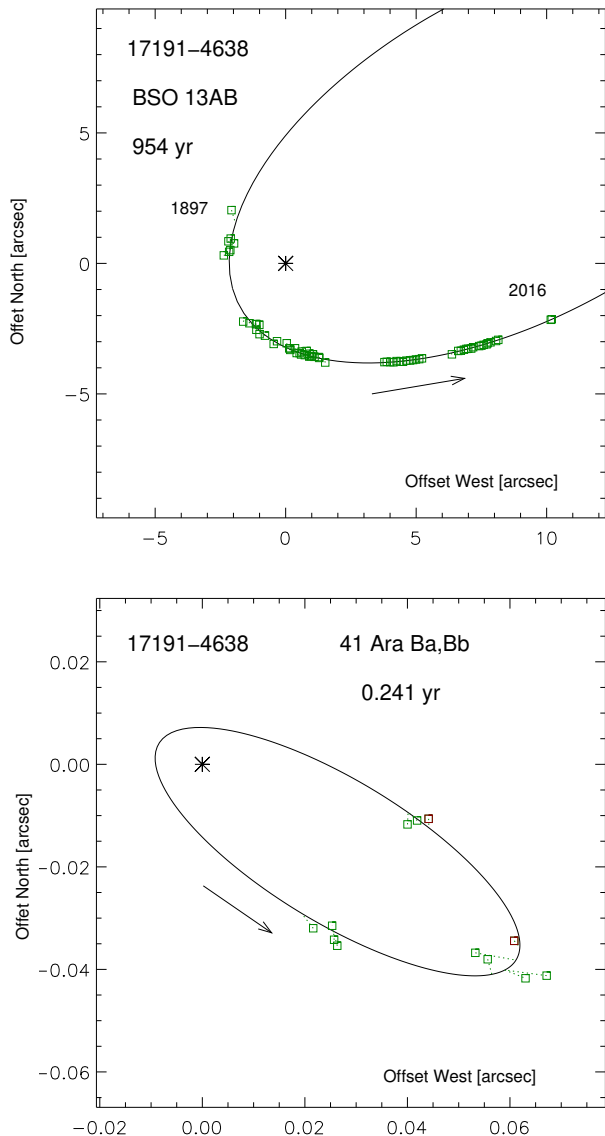


Figure 6. Orbits of the outer (top) and inner (bottom) pairs in 41 Ara.

The mutual inclination between orbits Φ , defined by the angles Ω and i , is known better than the uncertain period or eccentricity of the outer orbit. It is $\Phi = 107 \pm 2^\circ$ if the ascending node of the outer orbit is chosen correctly on the basis of the small RV difference between A and B. The alternative node corresponds to a mutual inclination of 48° . Therefore, to the best of our current knowledge, the inner and outer orbits in this triple system are almost orthogonal.

6. HIP 84720 (41 ARA)

The bright star 41 Ara (HR 6416, GJ 666A, WDS J17191-4638, G8/K0V) is located at 8 pc from the Sun.

Just like our nearest neighbor α Cen, this is a triple system. The outer pair A,B was first resolved at the end of the 19th century at $3''$ and presently it has opened up to $10''$, moving slowly on a millenium-long orbit. The secondary star B was announced as an 88 day spectroscopic binary by Raghavan et al. (2010), but its spectroscopic orbit has never been published. Recently, Gaia determined an astrometric orbit of this pair with the same period. The Gaia orbital solution also gives the unbiased parallax of 113.86 ± 0.03 mas, in excellent agreement with the parallax of star A (113.75 mas), and the unbiased PM. The Ba,Bb pair was tentatively resolved at SOAR in 2016 and was monitored since that time. Despite being relatively bright, it is a difficult target for speckle interferometry because the magnitude difference in the I band is substantial, 1.41 ± 0.11 mag, and the separation is always close to the diffraction limit. The orbit of Ba,Bb based on the SOAR data was announced in Tokovinin (2023b); it is updated here. The period and eccentricity are fixed to the values determined by Gaia. Figure 6 plots the inner and outer orbits.

Although the arc of the outer orbit covered by the measurements is relatively large and includes periastron, the orbit is not well constrained because several its elements are strongly correlated. Several orbits of A,B are found in the literature. Here only the more accurate photographic measures, available since 1931, are used, complemented by the less accurate earlier micrometer measures and the precise relative positions from Hipparcos and Gaia. This orbit is very similar to the 953 yr orbit computed by Scardia et al. (2013). On the other hand, the latest 609 yr orbit by Izmailov (2019), obtained via a formal fit to all data, is questionable. The estimated mass sum of A,B is $1.88 M_\odot$ (see below), larger but compatible with the mass sum deduced from the parallax of 113.8 mas and the outer orbit ($1.54 M_\odot$). If the outer eccentricity is forced to a slightly smaller value, e.g. 0.75, the mass sum of A,B increases and approaches the photometric estimate, while the period of A,B becomes shorter.

Jenkins et al. (2015) detected an RV trend in the star A from precise measurements with the HARPS and UCLES spectrometers. I used the latter data (provided by D. Rabout) because they cover a larger time span. Their RVs (in m s^{-1}) are determined with an arbitrary zero point. The fitted RV amplitude of A, 1.956 ± 0.067 km s^{-1} , matches the expectation and defines the true ascending node of the outer orbit, while the systemic velocity is meaningless. The RV amplitude corresponds to a mass of $0.97 M_\odot$ for B, assuming that A is $0.87 M_\odot$ (see below). So, the RV trend of star A detected by Jenkins et al. (2015) is caused by its motion in the

outer orbit. The rms residuals to the orbit are 4.3 m s^{-1} , while the quoted RV errors are around 1 m s^{-1} . The additional RV scatter, if proven to be real, can be caused by planets revolving around star A. Lacking permission from the authors, I do not reproduce the RVs of A in Table 4.

Adopting the magnitude difference $\Delta V_{\text{Ba,Bb}} = 1.75$ mag, I get the V magnitudes of Ba and Bb of 8.89 and 10.64 mag and estimate the masses as 0.60 and $0.41 M_{\odot}$ from the standard main-sequence relations (the spectral type of B is M0VpCa-3Cr-1). The inner orbit corresponds to the mass sum of $0.81 M_{\odot}$. The estimated masses of Ba and Bb imply the mass ratio $q_{\text{Ba,Bb}} = 0.68$. With a magnitude difference of ~ 1.5 mag in the G band, the light ratio is $r_{\text{Ba,Bb}} = 0.25$. The ratio of the astrometric amplitude, 9.3 mas (Gaia), to the full axis of Ba,Bb, 41.0 mas , gives the wobble factor $f^* = 0.23$, in excellent agreement with its estimate $f^* = q/(1+q) - r/(1+r) = 0.21$.

The inner semimajor axis is measured with a relative error of 0.06, which translates to the relative mass sum error of ~ 0.2 . Therefore, the constraint on the mass sum of Ba,Bb is weak, and this binary definitely cannot serve as a benchmark. However, the star is bright in the infrared and accessible to the VLTI interferometer. The RV of star B has been monitored in the past according to Raghavan et al. (2010), but these data remain unpublished. It will be easy to obtain a modern 88 day spectroscopic orbit of Ba,Bb. Combined with accurate relative positions from the VLTI, these data will constrain the masses in this pair.

7. HIP 89234 (HR 6751)

This bright ($V = 5.85$ mag, F5V) visual triple system is known as HR 6751 and WDS J18126–7340. The outer companion B (HDO 284AB) at $2''$ has been measured visually since 1891, although the available historic coverage of 7 micrometer measures is sparse. The inner subsystem Aa,Ab was discovered at SOAR in 2008 and is designated as TOK 58Aa,Ab. Both visual companions are fainter than star A by ~ 3.4 mag in the I band.

Gaia DR3 measured parallaxes of 23.678 ± 0.040 and 23.710 ± 0.035 for stars A and B, respectively, with a modest RUWE. During the Gaia mission, star A moved almost linearly in the inner orbit and Ab was at close separation, explaining why it has not spoiled the astrometry. The “photometric” masses of Aa, Ab, and B estimated from their absolute magnitudes are 1.46, 0.73, and $0.82 M_{\odot}$, respectively. Star A is slightly evolved (above the main sequence), and Abu-Alrob et al. (2023) estimated its age at 1.4 Gyr.

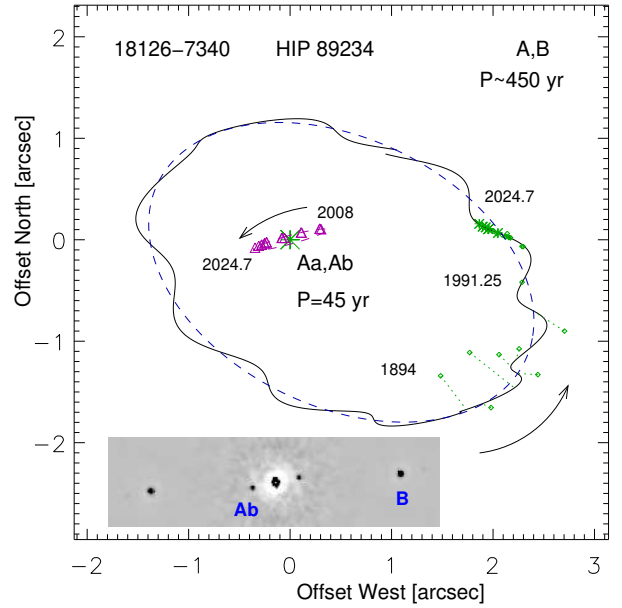


Figure 7. Orbits of HIP 89234. The insert shows the latest speckle ACF recorded in 2024.7 in negative rendering.

Ling (2016) published a preliminary (grade 5) orbit of A,B with a period of 324 yr. The small arc of this orbit covered so far gives only loose constraints on the elements. The inner subsystem is also observed over a fraction of its orbit. Here the position measurements are fitted by two Keplerian orbits simultaneously (Figure 7).

The measurements of the inner pair Aa,Ab come from SOAR, except one measure in 2017.44 made by Horch et al. (2019) at the Gemini-S telescope, where the quadrant of Aa,Ab had to be changed. The quadrants of all SOAR measures are defined by the orientation of the outer pair and cannot be changed. The pair Aa,Ab was discovered in 2008.77 at 288° position angle, went through conjunction in 2018, and now opens up at 99° . The free fit gives the inner eccentricity of 0.006 ± 0.025 , below significance, so the zero-eccentricity solution is imposed. The poorly constrained outer period is fixed to 450 yr and the outer eccentricity to 0.3 (this combination defines the remaining outer elements and matches the expected mass sum). The motion of B relative to Aa in 2016.0 predicted by both orbits is $(31.1, 12.4) \text{ mas yr}^{-1}$. The motion of B relative to the photocenter of A measured by Gaia DR3 is $(29.3, 12.3) \text{ mas yr}^{-1}$, in good agreement. Given the relatively large wobble amplitude $f = 0.37 \pm 0.02$, the speed of B relative to A depends on both orbits. The wobble factor indicates the inner mass ratio $q_{\text{in}} = 0.59$, and the photometric masses correspond to $q_{\text{in}} = 0.50$.

Using the Gaia parallax of Aa, the two orbits lead to the inner and outer mass sums of 2.0 and $3.0 M_{\odot}$, respectively. The estimated mass sums are 2.2 and 3.0

M_{\odot} . Considering the preliminary nature of both orbits, this agreement is satisfactory. I tried to impose different constraints on the outer orbit and found that the outer mass sum is relatively robust, and it can be even larger, e.g. $3.6 M_{\odot}$ if we set $e_{\text{out}} = 0.2$. This hints that star B may have a subsystem.

The different inclinations of the orbits are quite obvious (Figure 7). The mutual inclination computed from the elements is either 51° or 118° . Note also the modest period ratio, ~ 10 . Dynamical stability of this system (Mardling & Aarseth 2001) calls for $a_{\text{out}}(1 - e_{\text{out}})/a_{\text{in}} > 3.5$ or $e_{\text{out}} < 0.35$. Therefore, very eccentric outer orbits are excluded, justifying the adopted value of e_{out} .

8. HIP 105404 (BS IND)

This eclipsing triple system is designated in the catalogs as BS Ind, HD 202947, HIP 105404, TIC 79403459, WDS J21210–5229 ($V = 8.90$ mag, K0V). Literature suggests its membership in the Tucana-Horlogium association with an estimated age of ~ 30 Myr based on kinematics and such youth indicators as location on the color-magnitude diagrams, presence of the lithium line, and chromospheric activity. The triple nature of BS Ind has been discovered by Guenther et al. (2005). On the one hand, they found eclipses with a period of 0.435338 days using Hipparcos photometry. On the other hand, the RV variation indicated an eccentric orbit with a period of 3.3 yr and $e = 0.6$. These authors concluded that the RVs refer to the K0V primary star A of mass $0.9 M_{\odot}$, while the eclipsing pair of comparable total mass is hosted by the secondary component B. The RVs of Ba were measured approximately from the broad feature in the CCF, leading to an RV amplitude of 65 km s^{-1} for Ba. The authors suggested that the outer pair can be resolved interferometrically.

This star has been observed by the SOAR speckle camera in 2018 in a survey of young moving groups and resolved into a 90 mas pair with comparable components (Tokovinin et al. 2021). The WDS assigned it a meaningless name CVN 66Aa,Ab. Two faint companions B and C at $3''.25$ and $5''.86$ separations, denoted as CVN 66AB and AC, respectively, are optical, as evidenced by their Gaia parallaxes. Further speckle monitoring revealed a fast orbital motion. Speckle observations accumulated from 2018.8 to 2024.6 allow calculation of the combined spectro-interferometric orbit using the published RVs. New astrometry from Gaia and the photometry from TESS contribute additional information on this system.

The 14 speckle measurements and the available RVs were fitted by a Keplerian orbit (Figure 8). The weighted rms residuals are 1.4 mas in position and

0.28 km s^{-1} in RVs. The RVs were measured by Guenther et al. (2005) in 1994.7–2004.5 and, together with the recent speckle data, they accurately constrain the outer period of 3.3474 ± 0.0015 yr. I downloaded from the ESO archive three additional FEROS spectra taken in 2017.545 and computed the RV of 15.9 km s^{-1} by cross-correlation (note the first point on the descending branch of the RV curve). Three RVs measured with CHIRON in 2022–2024 were used as well. Although the orbit plots look good, there remain correlations between several elements (e.g. e and P) in the least-squares fit. A better spectroscopic coverage of the periastron is needed to reduce the correlations. Unfortunately, the periastron in 2023.9 was missed because CHIRON was closed at that time.

Motion of the photocenter with the 3.3 yr period biases the parallax and PM measurements from space missions. The HIP2 parallax (van Leeuwen 2007) is 22.25 ± 1.40 mas, the Gaia parallaxes are 18.99 ± 0.33 mas (DR2) and 16.50 ± 0.51 mas (DR3). Note the increased error of the DR3 parallax caused by the fast motion near periastron in 2017. The DR2 parallax is based on the orbit segment near the apastron and appears to be less biased. Using the mass sum of $2.2 M_{\odot}$ estimated from absolute magnitudes, I adopt the dynamical parallax of 19.0 mas, same as the DR2 parallax. With the A mass of $0.85 M_{\odot}$ (see below), the RV amplitude and inclination correspond to the B mass of $1.36 M_{\odot}$, matching the photometrically estimated mass sum of Ba,Bb.

The TESS light curves (LCs) measured in 2018 (sector 1) and 2020 (sector 27) are presented in the lower panels of Figure 8. These curves are not phase-folded. There are a few flares, as expected in these chromospherically active stars (flares were also detected previously from the ground). The flux normalization is approximate.

A striking difference between the 2018 and 2020 LCs is evident. The former has a depression before the secondary minimum and a hump after. Such features are attributed usually to an asymmetric accretion disk or a stream around the secondary, although they could also be caused by large starspots. The brighter part of the disk is eclipsed by the primary before the secondary minimum. The secondary minimum has a small flat bottom, signaling that the eclipse is total. Hence, the depth of the secondary minimum, 0.10, equals the relative flux of Bb in the TESS band. The primary eclipse is partial, so its depth of ~ 0.22 is a lower limit on the Ba relative flux (I adopt below 0.30). The Hipparcos LC published by Guenther et al. (2005) is noisy, but suggests a much smaller secondary minimum. This can be explained by the lower temperature of the secondary (less light in the Hipparcos band) and, possibly, a lower inclination of the

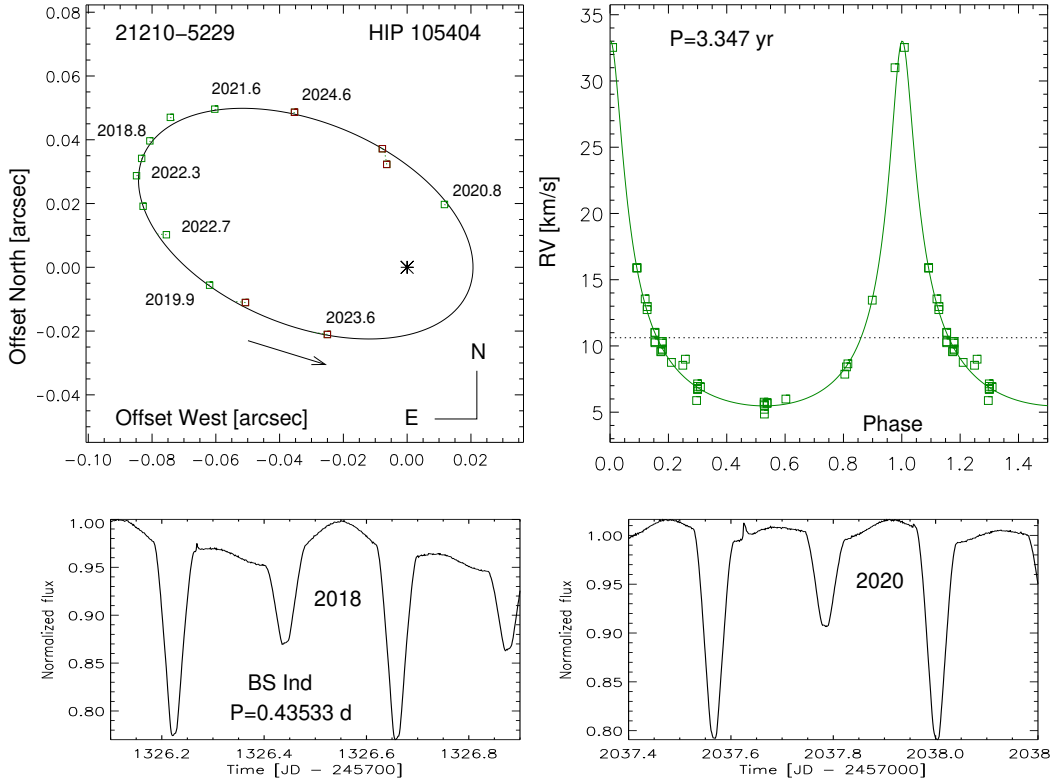


Figure 8. The outer orbit (top) and the TESS light curves (bottom) of BS Ind.

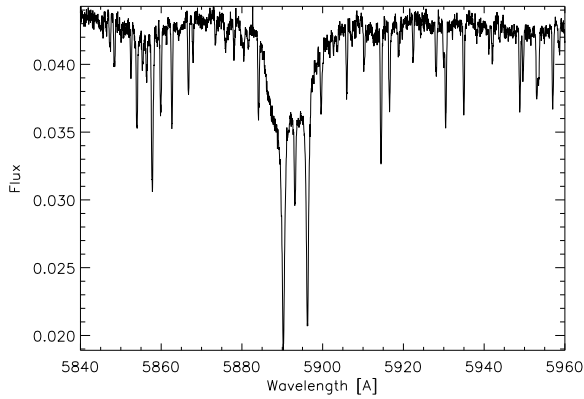


Figure 9. Fragment of the FEROS spectrum of BS Ind around sodium D lines taken on 2017-08-03. Note the narrow lines of A and the wide and blended lines of Ba and Bb. The spectrum was downloaded from the ESO archive. The flux units are arbitrary.

eclipsing pair due to its precession. The non-stationarity of the LC evidenced by TESS merits further investigation.

The magnitude difference between A and B measured at SOAR establishes the relative fluxes of A and B. It is 0.31 mag in I (7 measures, rms scatter 0.19 mag) and 0.40 mag in y (7 measures, rms scatter 0.50 mag).

Variability of star B increases the scatter of differential speckle photometry at SOAR.

In the following, I adopt the flux ratio A:Ba:Bb of 0.60:0.30:0.10 in the T or G bands, in rough agreement with the speckle photometry and the TESS LCs. The combined magnitudes recovered from Simbad are 8.90 (V), 8.52 (G), 7.89 (I), 7.18 (J), and 6.57 (K). Splitting the V flux in the indicated proportion (which is not quite correct, considering that B is redder than A) results in the V magnitudes of 9.46, 10.22, and 11.41 mag for A, Ba, and Bb, respectively. The parallax of 19 mas and the standard main-sequence relation lead to the masses of 0.86, 0.78, and 0.70 M_{\odot} . However, the RV amplitude of Ba measured by [Guenther et al. \(2005\)](#) imply the Bb mass of 0.23 M_{\odot} , while the outer orbit corresponds to the Bb mass of 0.60 M_{\odot} (subtracting the Ba mass 0.78 from the mass of B, 1.38). [Guenther et al. \(2005\)](#) likely underestimated the RV amplitude of Ba owing to blending.

[Guenther et al. \(2005\)](#) looked for the signatures of the secondary components in the spectrum and could not find any. They assumed that B hosts two similar late-M dwarfs that are much fainter than A. In fact, as we know now, the fluxes of A and B are comparable (ratio 0.6:0.4), and the masses of Ba and Bb are in the K-dwarf domain. A fragment of the FEROS spectrum near the sodium D lines shown in [Figure 9](#) makes it clear

that the lines of Ba and Bb are strong, but very wide and blended. A spectroscopic orbit of Ba,Bb can possibly be determined by modeling the blended spectra. An even more accurate orbit of B could be derived by photometry. The estimated outer axis of the B orbit is about $a \sin i \approx 0.7$ au, so a light-time effect of ~ 5 min is expected.

The Gaia DR3, released in June 2022, did not provide astrometric or spectroscopic orbit of the outer pair, despite its short period. As a substitute, we can study the PMA measured by Gaia DR2 (less biased than DR3, see above). The long-term PM deduced by Brandt (2018) is $(36.58, -103.74)$ mas yr $^{-1}$, in excellent agreement with the Tycho-2 long-term PM of $(35.4, -101.2)$ mas yr $^{-1}$. Subtracting the long-term HIP-DR2 PM from the DR2 Gaia PM yields the PMA of $(-5.96, +7.83)$ mas yr $^{-1}$. The orbital motion of B relative to A in 2015.5 was $(19.65, -31.08)$ mas yr $^{-1}$. Considering the approximate nature of this calculation, the agreement of the PMA direction with predictions from the orbit is encouraging. The ratio of PMA and orbital velocities gives the wobble factor $f^* = 0.27$. The mass ratio $q = 1.35/0.86 = 1.57$ and the light ratio $r = 0.4/0.6 = 0.67$ correspond to $f^* = 0.21$, in reasonable agreement. Therefore, the preliminary estimates of masses and relative fluxes given above are supported by the Gaia astrometry.

Guenther et al. (2005) drew attention to the fact that the Ba,Bb pair is the closest among known young binaries. Most eclipsing binaries with such short periods are older than ~ 0.6 Gyr, being produced by the slow angular momentum loss through stellar wind (e.g. Hwang & Zakamska 2020). However, the young age of BS Ind based on its assumed membership in the Tucana-Horlogium association may be incorrect. The long-term PM, center-of-mass RV, and parallax of 19.0 mas correspond to the Galactic velocity of $(U, V, W) = (-2.1, -27.6, -9.8)$ km s $^{-1}$ for BS Ind, while the mean velocity of the association is $(U, V, W) = (-10.72, -20.2, -0.7)$ km s $^{-1}$ (Gagné et al. 2018). The difference largely exceeds both the measurement errors and the velocity dispersion in the association. In fact, Guenther et al. (2005) already noted the large discrepancy between the mean RVs of BS Ind and Tuc-Hor, but, nevertheless, highlighted membership in the association in the title of their paper. The high chromospheric activity of BS Ind (emission lines, X-ray radiation, flares) could be maintained by the fast rotation in the synchronized pair Ba,Bb. A similar case of HIP 45734 containing a 0.5 day subsystem was studied by Tokovinin (2020): this object, believed to be a pre-main sequence star, in fact is older. On the other hand, Guenther et al. (2005) detected lithium lines in the spectrum, confirm-

ing the relative youth of BS Ind. The 2017 FEROS spectra contain a strong and narrow Li line, but the H α line is in absorption, with only a weak emission core at the center. The projected rotation velocity of A is modest, $V \sin i = 13.0 \pm 0.4$ km s $^{-1}$. This triple system is definitely not very old, but rather “juvenile”.

The large inclination of the outer orbit, 42° , excludes its coplanarity with the inner eclipsing pair. Dynamical interaction between the orbits should cause precession of the inner pair with a period on the order of $P_{\text{out}}^2/P_{\text{in}} \sim 850$ yr, or 4° in 10 yr, so a changing depth of the LC minima can possibly be detected. Furthermore, the eclipse time variation caused by the light-time effect and mutual dynamics can provide additional constraints on this interesting triple system.

9. SUMMARY

This work increases the number of nearby hierarchical systems with known orbits by a small amount, adding 10 orbits in 6 systems. The progress in this area is slow owing to such factors as required angular resolution and time coverage. I used the time series of speckle interferometry measurements at the 4.1 m SOAR telescope, complemented by RVs and other data available in the literature. These data give access to periods on the order of a decade (the 44 yr inner orbit is covered only partially). Longer periods of outer systems are determined with a large uncertainty using historic data, or simply estimated from projected separations. Figure 1 illustrates the wide range of periods addressed in this paper, from the shortest 0.5 day inner period of BS Ind to the longest 0.5 Myr outer period of HIP 11783.

Of special interest are two resolved triples with comparable separations and periods, HIP 64836 (5 yr and 30 yr) and HIP 89234 (45 yr and ~ 450 yr). The small period ratios (6 and 10) place these systems near the limit of dynamical stability. Hence dynamical interactions between inner and outer subsystems are strong and will eventually become measurable through deviations from the simple model of two Keplerian orbits used here. Period ratios close to integer numbers are suggestive of the mean motion resonances, but a complete coverage of outer orbits is needed to prove this hypothesis. It looks plausible for HIP 64836, where the orbits are near-circular and close to coplanarity. This systems joins the class of hierarchies with planetary-type architecture, presumably formed by fragmentation and migration in protostellar disks (Tokovinin 2021c). Other members of this class were discovered and/or studied by our team (Tokovinin et al. 2015; Tokovinin & Latham 2017; Tokovinin 2018c; Tokovinin & Latham 2020). The large mutual inclination of orbits in HIP 89234 sets

it apart from the planetary-type hierarchies, although small eccentricities match this architecture better than predictions for dynamically formed triples, where large eccentricities and misaligned orbits are expected.

Another system of interest is HIP 105404 (BS Ind). It is compact (outer period 3.3 yr), and such hierarchies are intrinsically rare. Its inner eclipsing pair is definitely misaligned with the well-defined outer orbit ($i_{\text{out}} = 42^\circ.3$), suggesting that Lidov-Kozai cycles coupled with tidal friction could have played a role in shrinking the inner pair. This system is not a member of the Tucana-Horlogium association, contrary to the belief of its discoverers (Guenther et al. 2005); signs of youth are attributable to the chromospheric activity of the tidally synchronized eclipsing pair.

The Gaia space mission will provide a time coverage of 11 yr in its final DR5, while its spatial resolution is limited to $0''.1$ by the 1 m apertures. The systems studied here take advantage of the accurate Gaia astrometry and also reveal its limitations. Standard astrometric models (single star, binary orbit, acceleration) do not capture complex motions in some close triple systems. Dedicated analysis of individual transits (to become public in DR4) will be greatly helped by additional ground-based

data such as speckle interferometry and high-resolution spectroscopy.

I am grateful to D. Latham for providing the RVs of HD 130412 measured at CfA and for comments on the paper. The research was funded by the NSF's NOIRLab. This work used the SIMBAD service operated by Centre des Données Stellaires (Strasbourg, France), bibliographic references from the Astrophysics Data System maintained by SAO/NASA, and the Washington Double Star Catalog maintained at USNO. This work has made use of data from the European Space Agency (ESA) mission Gaia (<https://www.cosmos.esa.int/gaia>), processed by the Gaia Data Processing and Analysis Consortium (DPAC, <https://www.cosmos.esa.int/web/gaia/dpac/consortium>). Funding for the DPAC has been provided by national institutions, in particular the institutions participating in the Gaia Multilateral Agreement. This research has made use of the services of the ESO Science Archive Facility and data collected by the TESS mission funded by the NASA Explorer Program.

Facility: SOAR, CTIO:1.5m, Gaia, TESS

REFERENCES

- Abu-Alrob, E. M., Hussein, A. M., & Al-Wardat, M. A. 2023, *AJ*, 165, 221, doi: [10.3847/1538-3881/acc9ab](https://doi.org/10.3847/1538-3881/acc9ab)
- Brandt, T. D. 2018, *ApJS*, 239, 31, doi: [10.3847/1538-4365/aaec06](https://doi.org/10.3847/1538-4365/aaec06)
- Burnham, S. W. 1875, *Astronomische Nachrichten*, 86, 337, doi: [10.1002/asna.18750862202](https://doi.org/10.1002/asna.18750862202)
- Gagné, J., Mamajek, E. E., Malo, L., et al. 2018, *ApJ*, 856, 23, doi: [10.3847/1538-4357/aaae09](https://doi.org/10.3847/1538-4357/aaae09)
- Gaia Collaboration, Arenou, F., Babusiaux, C., et al. 2022, arXiv e-prints, arXiv:2206.05595, <https://arxiv.org/abs/2206.05595>
- Gaia Collaboration, Brown, A. G. A., Vallenari, A., et al. 2021, *A&A*, 649, A1, doi: [10.1051/0004-6361/202039657](https://doi.org/10.1051/0004-6361/202039657)
- . 2016, *A&A*, 595, A2, doi: [10.1051/0004-6361/201629512](https://doi.org/10.1051/0004-6361/201629512)
- Guenther, E. W., Covino, E., Alcalá, J. M., Esposito, M., & Mundt, R. 2005, *A&A*, 433, 629, doi: [10.1051/0004-6361:20042291](https://doi.org/10.1051/0004-6361:20042291)
- Horch, E. P., Bahi, L. A. P., Gaulin, J. R., et al. 2012, *AJ*, 143, 10, doi: [10.1088/0004-6256/143/1/10](https://doi.org/10.1088/0004-6256/143/1/10)
- Horch, E. P., van Belle, G. T., Davidson, James W., J., et al. 2015, *AJ*, 150, 151, doi: [10.1088/0004-6256/150/5/151](https://doi.org/10.1088/0004-6256/150/5/151)
- Horch, E. P., Casetti-Dinescu, D. I., Camarata, M. A., et al. 2017, *AJ*, 153, 212, doi: [10.3847/1538-3881/aa6749](https://doi.org/10.3847/1538-3881/aa6749)
- Horch, E. P., Tokovinin, A., Weiss, S. A., et al. 2019, *AJ*, 157, 56, doi: [10.3847/1538-3881/aaf87e](https://doi.org/10.3847/1538-3881/aaf87e)
- Hwang, H.-C., & Zakamska, N. L. 2020, *MNRAS*, 493, 2271, doi: [10.1093/mnras/staa400](https://doi.org/10.1093/mnras/staa400)
- Izmailov, I. S. 2019, *Astronomy Letters*, 45, 30, doi: [10.1134/S106377371901002X](https://doi.org/10.1134/S106377371901002X)
- Jenkins, J. S., Díaz, M., Jones, H. R. A., et al. 2015, *MNRAS*, 453, 1439, doi: [10.1093/mnras/stv1596](https://doi.org/10.1093/mnras/stv1596)
- Kaufer, A., & Pasquini, L. 1998, in *Society of Photo-Optical Instrumentation Engineers (SPIE) Conference Series*, Vol. 3355, *Optical Astronomical Instrumentation*, ed. S. D'Odorico, 844–854, doi: [10.1117/12.316798](https://doi.org/10.1117/12.316798)
- Lee, A. T., Offner, S. S. R., Kratter, K. M., Smullen, R. A., & Li, P. S. 2019, *ApJ*, 887, 232, doi: [10.3847/1538-4357/ab584b](https://doi.org/10.3847/1538-4357/ab584b)
- Ling, J. 2016, *IAU Commission 26 Information Circular*, 189, 1
- Makarov, V. V., & Kaplan, G. H. 2005, *AJ*, 129, 2420, doi: [10.1086/429590](https://doi.org/10.1086/429590)
- Mardling, R. A., & Aarseth, S. J. 2001, *MNRAS*, 321, 398, doi: [10.1046/j.1365-8711.2001.03974.x](https://doi.org/10.1046/j.1365-8711.2001.03974.x)
- Mason, B. D., Wycoff, G. L., Hartkopf, W. I., Douglass, G. G., & Worley, C. E. 2001, *AJ*, 122, 3466, doi: [10.1086/323920](https://doi.org/10.1086/323920)

- Nordström, B., Mayor, M., Andersen, J., et al. 2004, *A&A*, 418, 989, doi: [10.1051/0004-6361:20035959](https://doi.org/10.1051/0004-6361:20035959)
- Offner, S. S. R., Moe, M., Kratter, K. M., et al. 2023, in *Astronomical Society of the Pacific Conference Series*, Vol. 534, *Protostars and Planets VII*, ed. S. Inutsuka, Y. Aikawa, T. Muto, K. Tomida, & M. Tamura, 275, doi: [10.48550/arXiv.2203.10066](https://doi.org/10.48550/arXiv.2203.10066)
- Pecaut, M. J., & Mamajek, E. E. 2013, *ApJS*, 208, 9, doi: [10.1088/0067-0049/208/1/9](https://doi.org/10.1088/0067-0049/208/1/9)
- Raghavan, D., McAlister, H. A., Henry, T. J., et al. 2010, *ApJS*, 190, 1, doi: [10.1088/0067-0049/190/1/1](https://doi.org/10.1088/0067-0049/190/1/1)
- Ricker, G. R., Winn, J. N., Vanderspek, R., et al. 2014, in *Society of Photo-Optical Instrumentation Engineers (SPIE) Conference Series*, Vol. 9143, *Space Telescopes and Instrumentation 2014: Optical, Infrared, and Millimeter Wave*, ed. J. Oschmann, Jacobus M., M. Clampin, G. G. Fazio, & H. A. MacEwen, 914320, doi: [10.1117/12.2063489](https://doi.org/10.1117/12.2063489)
- Scardia, M., Prieur, J.-L., Pansecchi, L., & Argyle, R. 2013, *IAU Commission 26 Information Circular*, 281, 1
- Soubiran, C., Le Campion, J. F., Cayrel de Strobel, G., & Caillo, A. 2010, *A&A*, 515, A111, doi: [10.1051/0004-6361/201014247](https://doi.org/10.1051/0004-6361/201014247)
- Sperauskas, J., Bartasiūtė, S., Boyle, R. P., et al. 2016, *A&A*, 596, A116, doi: [10.1051/0004-6361/201527850](https://doi.org/10.1051/0004-6361/201527850)
- Steinmetz, M., Guiglion, G., McMillan, P. J., et al. 2020, *AJ*, 160, 83, doi: [10.3847/1538-3881/ab9ab8](https://doi.org/10.3847/1538-3881/ab9ab8)
- Szentgyorgyi, A. H., & Furész, G. 2007, in *Revista Mexicana de Astronomia y Astrofisica Conference Series*, Vol. 28, *Revista Mexicana de Astronomia y Astrofisica Conference Series*, ed. S. Kurtz, 129–133
- Takeda, Y., Sato, B., Kambe, E., et al. 2005, *PASJ*, 57, 13, doi: [10.1093/pasj/57.1.13](https://doi.org/10.1093/pasj/57.1.13)
- Tokovinin, A. 2016, *AJ*, 152, 11, doi: [10.3847/0004-6256/152/1/11](https://doi.org/10.3847/0004-6256/152/1/11)
- . 2017, *ORBIT3: Orbits of Triple Stars*, Zenodo, doi: [10.5281/zenodo.321854](https://doi.org/10.5281/zenodo.321854)
- . 2018a, *ApJS*, 235, 6, doi: [10.3847/1538-4365/aaa1a5](https://doi.org/10.3847/1538-4365/aaa1a5)
- . 2018b, *PASP*, 130, 035002, doi: [10.1088/1538-3873/aaa7d9](https://doi.org/10.1088/1538-3873/aaa7d9)
- . 2018c, *AJ*, 155, 160, doi: [10.3847/1538-3881/aab102](https://doi.org/10.3847/1538-3881/aab102)
- . 2020, *AJ*, 159, 88, doi: [10.3847/1538-3881/ab6a13](https://doi.org/10.3847/1538-3881/ab6a13)
- . 2021a, *AJ*, 161, 144, doi: [10.3847/1538-3881/abda42](https://doi.org/10.3847/1538-3881/abda42)
- . 2021b, *IAU Commission 26 Information Circular*, 203, 1
- . 2021c, *Universe*, 7, 352, doi: [10.3390/universe7090352](https://doi.org/10.3390/universe7090352)
- . 2023a, *AJ*, 165, 165, doi: [10.3847/1538-3881/acbf32](https://doi.org/10.3847/1538-3881/acbf32)
- . 2023b, *IAU Commission 26 Information Circular*, 209, 1
- Tokovinin, A., Fischer, D. A., Bonati, M., et al. 2013, *PASP*, 125, 1336, doi: [10.1086/674012](https://doi.org/10.1086/674012)
- Tokovinin, A., & Latham, D. W. 2017, *ApJ*, 838, 54, doi: [10.3847/1538-4357/aa6331](https://doi.org/10.3847/1538-4357/aa6331)
- . 2020, *AJ*, 160, 251, doi: [10.3847/1538-3881/abbad4](https://doi.org/10.3847/1538-3881/abbad4)
- Tokovinin, A., Latham, D. W., & Mason, B. D. 2015, *AJ*, 149, 195, doi: [10.1088/0004-6256/149/6/195](https://doi.org/10.1088/0004-6256/149/6/195)
- Tokovinin, A., Mason, B. D., & Hartkopf, W. I. 2010, *AJ*, 139, 743, doi: [10.1088/0004-6256/139/2/743](https://doi.org/10.1088/0004-6256/139/2/743)
- Tokovinin, A., Mason, B. D., Mendez, R. A., & Costa, E. 2022, *AJ*, 164, 58, doi: [10.3847/1538-3881/ac78e7](https://doi.org/10.3847/1538-3881/ac78e7)
- . 2024, *AJ*, 168, 28, doi: [10.3847/1538-3881/ad4d56](https://doi.org/10.3847/1538-3881/ad4d56)
- Tokovinin, A., Mason, B. D., Mendez, R. A., et al. 2021, *AJ*, 162, 41, doi: [10.3847/1538-3881/ac00bd](https://doi.org/10.3847/1538-3881/ac00bd)
- van Leeuwen, F. 2007, *A&A*, 474, 653, doi: [10.1051/0004-6361:20078357](https://doi.org/10.1051/0004-6361:20078357)